Japanese Journal of Applied Physics
Vol. 44, No. 11, 2005, pp. 8082–8085

Dynamic Stability of Liquid Crystal Depending on Shape of Pixel Edge in the Fringe Field Switching Mode

M. S. KIM[1,2]*, S. M. SEEN[1], Y. H. JUNG[1], H. Y. KIM[1,2], S. Y. KIM[1], K. H. LEE[1], Y. J. LIM[1] and S. H. LEE[2]

[1]*SBU Development Center, BOE_TFT_LCD_SBU, San 136-1, Ami-ri, Bubal-eup, Ichon-si, Kyungki-do 467-701, Korea*
[2]*School of Advanced Materials Engineering, Chonbuk National University, Chonju-si, Chonbuk 561-756, Korea*

(Received May 4, 2005; accepted June 30, 2005; published November 9, 2005)

We studied the voltage–dependent liquid crystal (LC) dynamic stability corresponding to the pixel edge shape in the fringe field switching (FFS) mode. LC dynamics is very unstable near the edge of the pixel slit, where there is a horizontally different field direction compared with the active region, particularly when the slit angle decreases to 3°. Actually, there are strong field competitions near the edge of the pixel slit due to the patterned pixel shape. Also, a dark disclination line (D/L) at the domain boundary is generated with increasing operation voltage and the D/L extends into the active area at a high applied voltage. It is possible to control LC dynamics near the pixel edge by using different pixel edge shapes. In this paper, we propose an advanced edge shape. This shape has no reverse twist region, unlike the conventional structure, and therefore, LC dynamics is very stable near the edge of the pixel slit. This result indicates that a pixel edge shape with no reverse twist is very important in the design of a high-image-quality FFS mode. [DOI: 10.1143/JJAP.44.8082]

KEYWORDS: reverse twist, fringe field switching, dynamic stability

1. Introduction

Today, liquid crystal displays (LCDs) with a wide viewing technique are in various applications from mobile phones, notebook personal computers (NBPCs) to television (TV) products. The in-plane switching (IPS)[1,2] mode with a wide viewing technique is the first mode to exhibit high image quality, although it shows intrinsically low transmittance. On the other hand, the fringe field switching (FFS) mode,[3,4] which is driven by a fringe electric field, is representative of modes that simultaneously shows high transmittance and wide viewing characteristics. Actually, in the FFS mode using the LC with positive dielectric anisotropy, the horizontally field direction of the active region is different from the edge of the pixel slit owing to the patterned pixel edge shape. Thus the LC dynamics near the edge of the pixel slit becomes very unstable upon the application of an external pressure or a high voltage. This phenomenon is notable when the slit angle of the pixel decreases. For the application to pressure-sensitive pen-based displays, it is necessary to obtain external pressure-resistance or voltage-independent LC dynamic stability.[5,6] It is also important for obtaining good electrooptic characteristics such as low driving voltage and high transmittance.

To solve this problem, in this study we propose an advanced pixel edge shape structure with good dynamic stability in the FFS mode. We also investigate the electro-optic characteristics and dynamic stability of the LC director by three-dimensional simulation.

2. Simulation and Experimental Results

Figure 1 shows a top view of the structure in the FFS mode with the LCs in the off and on states. First, an indium/tin oxide (ITO) layer with a thickness of 400 Å was deposited on the bottom glass substrate, and then a passivation layer, SiO_2, with a thickness of 3000 Å was coated by chemical vapor deposition. Finally, another ITO layer with a thickness of 400 Å was deposited and patterned as interdigital electrodes. The width of the second ITO layer electrodes was 3 μm, the distance between the electrodes was 5 μm, and the slit angle (SA) of the second ITO was θ. There was no electrode on the top glass substrate. In this case, the first and second ITO layers functioned as common and pixel electrodes, respectively, and there was no distance between the first and second ITO layers along the horizontal y direction, so that a fringe electric field is generated with a bias voltage. At that time, the horizontally fringe electric field direction for the active region was different from the edge of the pixel slit due to the patterned pixel edge shape, as shown in Fig. 1. The alignment layer was coated on both substrates and rubbing was performed in antiparallel directions. The rubbing angle was defined as the angle with respect to the horizontal component of the fringe field (E_x). The pretilt angle generated by rubbing was 2°. The two glass substrates were then assembled to provide a cell gap (d) of 3.6 μm. The liquid crystal with a positive dielectric anisotropy ($\Delta n = 0.098$ at $\lambda = 589$ nm, $\Delta\epsilon = 8.2$) from Merck was used in our experiments and simulations.

Two polarizers are oriented to cross each other with one of them being aligned parallel to the rubbing direction. In this case, the normalized transmission of light is given by

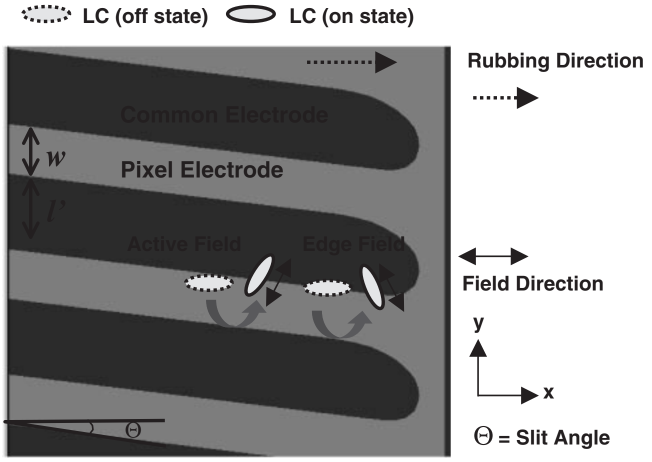

Fig. 1. Top view of the structure in the FFS mode with electric field direction.

---

*E-mail address: misuk7287@boehydis.com

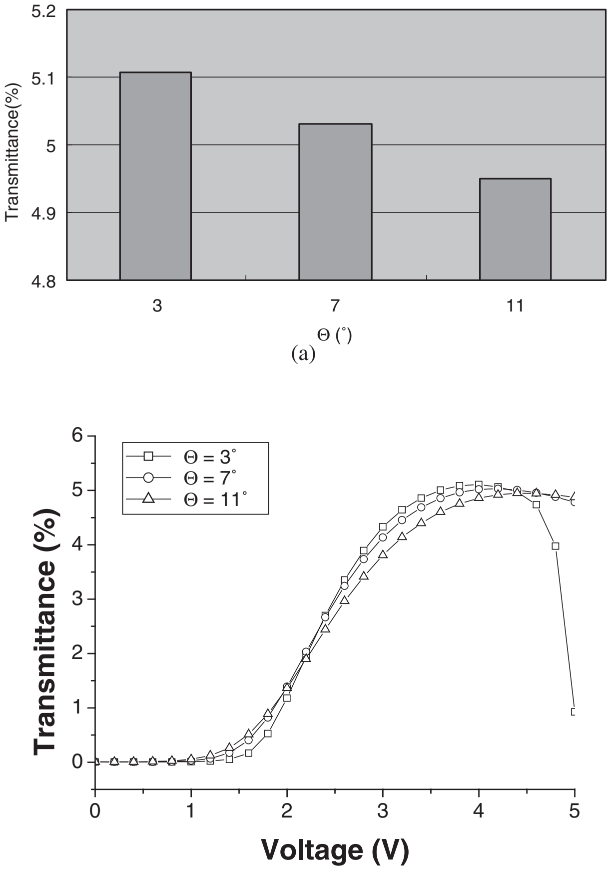

(a)

(b)

Fig. 2. (a) Experimental maximum transmittance graphs and (b) voltage–dependent transmittance curves of the FFS mode for various slit angles.

$$T/T_0 = \sin^2(2\psi)\sin^2(\pi d\Delta n/\lambda),$$

where ψ is the angle between the polarizer and the liquid crystal director. Therefore, the FFS mode is a normally black mode and the transmission becomes maximal when the LC director is rotated 45° by applying a voltage, given the birefringence of the LC medium.

Figure 2(a) shows the experimental maximum transmittance according to the slit angle in the FFS mode. As indicated in Fig. 2(a), the maximum transmittance at the operation voltage (V_{op}) increases as the slit angle decreases. This simply indicates that the ψ value becomes close to 45° while the slit angle decreases such that the maximum transmittance at V_{op} increases. Figure 2(b) shows experimental voltage–dependent transmittance (V–T) curves of the FFS mode. As seen in Fig. 2(a), the transmittance increases as the slit angle decreases but surprisingly, the transmittance rapidly decreases above V_{op} when the slit angle is 3°. To understand what is occurring inside the panel when the slit angle is 3°, we have observed the LC texture using the optical polarizing microscope with and above V_{op}, as shown in Fig. 3. As indicated in Fig. 3(a), the dark disclination lines occur at the pixel edge, which has a different field direction compared with the active area with V_{op}. The disclination lines extend into the active region with further increase of the voltage up to 5 V, as shown in Fig. 3(b). Therefore the transmittance in the panel dramatically decreases above V_{op}. We performed a computer simulation to analyze the phenomenon in detail. We used the commercially available software "Techwiz LCD" (Sanayisystem, Korea), where the motion of the LC director is calculated based on the Eriksen–Leslie theory and a 2 × 2 Jones matrix[7)] is applied for optical transmittance calculation.

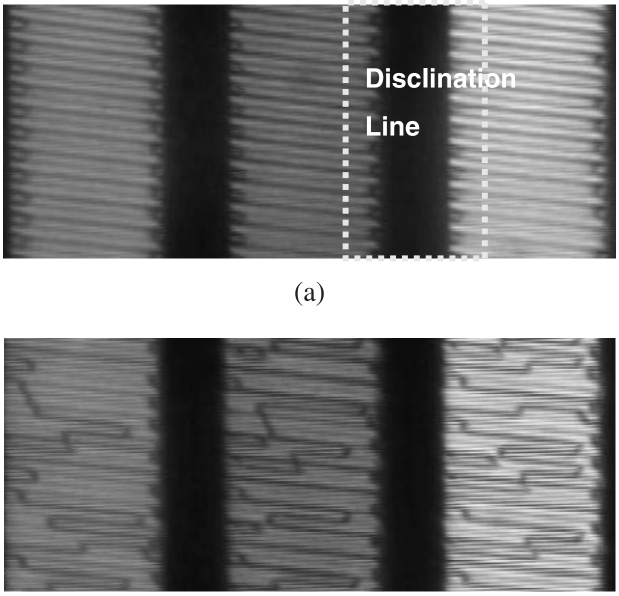

(a)

(b)

Fig. 3. Images of the FFS mode showing how the disclination lines extend into the active area from the domain boundary region: (a) with V_{op} and (b) above V_{op}.

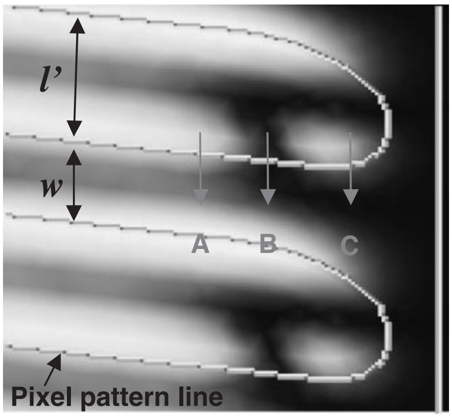

Fig. 4. Simulational transmittance result when slit angle is 3°.

Figure 4 shows the transmittance of the pixel electrodes with V_{op}, where A, B and C indicate the adjacent active region, the dark disclination region and the edge of the pixel slit, respectively. As seen in Fig. 4, the dark disclination lines exist at the boundary between A and C. This indicates that there is competition between the horizontal electric field at A and the horizontal electric field at C. Therefore the LC molecules existing in the domain, that is, B, cannot rotate in either direction and thus LC remains at the original state, giving rise to dark disclination lines.

Next, we analyze the profile of the LC director to observe the vicinity of the edge of the pixel slit in detail. Figure 5

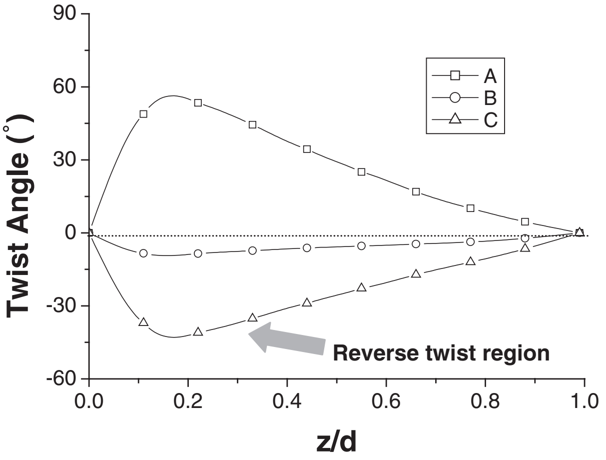

Fig. 5. Profile of twist angle of LC near the edge of pixel slit.

shows the twist angle of the LC along the vertical axis, which is the z direction, near the edge of the pixel slit when the applied voltage is V_{op}. The maximum twist angle at A is 57° near z/d of 0.2. That at B is $-2°$ near z/d of 0.1 and that at C is $-41°$ near z/d of 0.2. The above result shows that the twist direction at A is different from that at C, and LC molecules at C, which has a different field direction along the horizontal axis compared with the active region, undergo reverse twist. Therefore, LC molecules near C are very unstable. We also found that the twist angle is nominal at B which is the boundary between them such that dark disclination lines exist. Actually, the field competition near the edge of the pixel slit is large above V_{op} and disclination lines at B easily extend into the active region due to the strong reverse twist force. That is, dark disclination lines, which exist at the domain boundary, permeate into the active region, resulting in low transmittance when the slit angle is 3°. Therefore, we can understand that the design of a pixel slit with no reverse twist region is very important for obtaining the stable LC dynamics against high voltage.

We proposed an advanced FFS pixel slit structure in this paper. As shown in Fig. 6, C region of this structure does not cause transmittance by the reverse twist region unlike C region of the conventional structure. The reason is that the slit angle near the pixel edge is larger than the active slit angle such that reverse twist force generated due to horizontally different field directions does not exist. The slit angles of near the pixel edge and in the active region are defined as θ_{A} and θ_{E}, respectively.

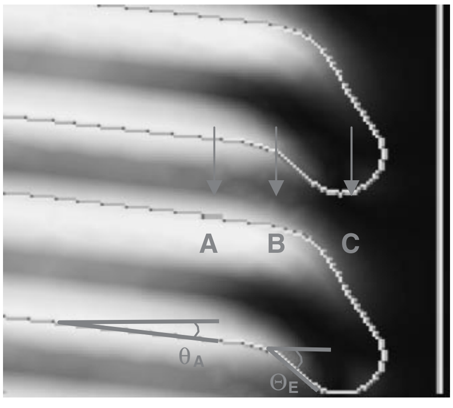

Fig. 6. Simulational transmittance result for advanced pixel edge shape.

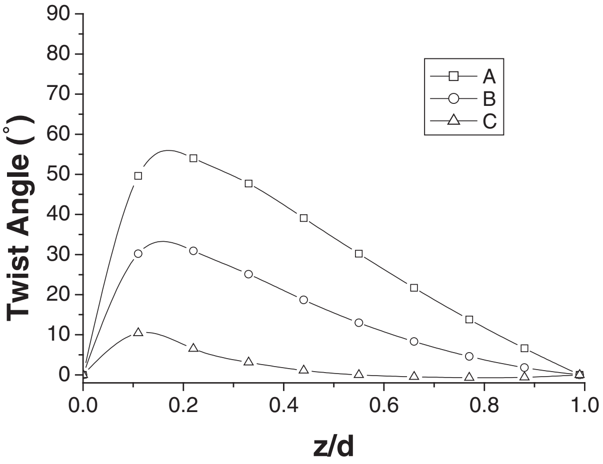

Fig. 7. Profile of twist angle of LC near edge of pixel slit for advanced pixel edge shape.

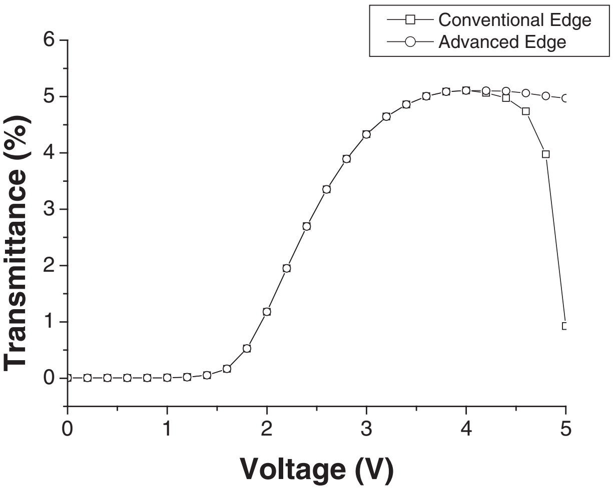

Fig. 8. Experimental voltage–dependent transmittance curves with different pixel edge shapes.

Figure 7 shows the profile of the LC director with the advanced pixel edge shape. As seen, there is no reverse twist at any position. Therefore, LC dynamics near the edge of pixel slit with the high applied voltage is very stable although the slit angle is 3°.

Figure 8 shows the experimental voltage–dependent transmittance curve for different pixel edge shapes when the slit angle is 3°. As shown, with the advanced edge shape structure, transmittance remains in the panel whereas transmittance in the conventional structure drops rapidly with increasing voltage up to 5 V. Therefore, voltage–dependent LC dynamic stability with the advanced edge shape structure is superior.

3. Summary

We studied the voltage–dependent LC dynamic stability with respect to the pixel edge shape in the FFS mode. LC dynamics is very unstable near the edge of the pixel slit, where there is a horizontally different field direction compared with the active region, particularly when the slit angle decreases to 3°. Dark disclination lines exist at the domain boundary while there are strong competitive forces between the two fields with V_{op}. The reverse twist force generated near the edge of the pixel slit is strong above V_{op}. Therefore, LC molecules near the edge of the pixel slit became very unstable and the disclination lines extended into the active area. Actually, it is possible to control LC dynamics near the pixel edge by changing pixel shape. The advanced edge structure for which the edge slit angle is larger than the active slit angle has no reverse twist region. Therefore LC dynamics is very stable near the pixel edge. This result indicates that the pixel edge shape with no reverse twist is very important in the design of the high-image-quality FFS mode. It is also useful for applications in external pressure-sensitive touch displays because voltage–dependent LC dynamics for such a structure will be very stable.

1) S.-K. Lee, Y. H. Jeung and D. S. Seo: Trans. EEM **4** (2003) 7.
2) H. Y. Kim, I. S. Song and S. H. Lee: Trans. EEM **4** (2003) 24.
3) S. H. Jung, H. Y. Kim, J.-H. Kim, S.-H. Nam and S. H. Lee: Jpn. J. Appl. Phys. **43** (2004) 1028.
4) M. S. Kim, Y. H. Jung, S. M. Seen, H. Y. Kim, S. Y. Kim, Y. J. Lim and S. H. Lee: Jpn. J. Appl. Phys. **44** (2005) 3121.
5) J. D. Noh, H. Y. Kim, J. M. Kim, J. W. Koh, H. S. Park and S. H. Lee: Proc. 2nd IDMC, 2002, p. 447.
6) H. Y. Kim, S. H. Nam and S. H. Lee: Jpn. J. Appl. Phys. **42** (2003) 2752.
7) A. Lien: Appl. Phys. Lett. **57** (1990) 2767.